Hindawi Publishing Corporation
Journal of Nanotechnology
Volume 2011, Article ID 507692, 6 pages
doi:10.1155/2011/507692

Research Article

Synthesis, Characterization and Catalytic Performance of $H_3SiW_{12}O_{40}/SiO_2$ Prepared by Sol-Gel Technique

W. N. R. W. Isahak,[1,2] M. Ismail,[2] N. M. Nordin,[1] J. M. Jahim,[2] and M. A. Yarmo[1]

[1] *Department of Chemical and Process Engineering, Faculty of Engineering and Built Environment, Universiti Kebangsaan Malaysia, 43600 Bangi, Malaysia*
[2] *School of Chemical Sciences and Food Technology, Faculty of Science and Technology, Universiti Kebangsaan Malaysia, 43600 Bangi, Malaysia*

Correspondence should be addressed to W. N. R. W. Isahak, wannorroslam@yahoo.com

Received 29 March 2011; Accepted 12 July 2011

Academic Editor: Mallikarjuna Nadagouda

The purpose of this work is to study the synthesis, characterization, and catalytic performance of two types of solid heteropoly acid catalysts, namely, silicotungstic acid bulk (STAB) and STA-silica sol-gel (STA-SG) compared with sulfuric acid. From the XPS analyses, there was a significant formation of W-O-Si, W-O-W, and Si-O-Si bonding in STA-SG compared to that in STAB. The main spectra of O1s (90.74%, 531.5 eV) followed by other O1s peak (9.26%, 532.8 eV) were due to the presence of W-O-W and W-O-Si bonds, respectively. The STA-SG catalyst was found to be the more environmentally benign solid acid catalyst for the esterification reaction between oleic acid and glycerol due to its lower toxicity supported by silica via sol-gel technique. In addition, the ease of separation for STA-SG catalyst was attributed to its insoluble state in the product phase. The esterification products were then analysed by FTIR and HPLC. Both the H_2SO_4 and the STAB gave high conversion of 100% and 98% but at a lower selectivity of GME with 81.6% and 89.9%, respectively. On the contrary, the STA-SG enabled a conversion of 94% but with a significantly higher GME selectivity of 95%, rendering it the more efficient solid acid catalyst.

1. Introduction

During the recent years, glycerol has been used as combustion materials around the world. The glycerol usage was expanded into many other high-quality products such as pharmaceutical, foods, and engine lubricant. To date, glycerol modification into glycerol monoester (GME) as lubrication materials that was based on the biosources was not really practised in the industry. The nature of the polar head group and the structure of the hydrocarbon tail of GME gave the strong impact as a friction reducer [1].

The GME is synthesized at present by acid catalyzed esterification of glycerol and fatty acids [2, 3]. Recently, list of studies involving alternative heterogeneous catalytic routes have been reported such as the glycerol esterification with lauric acid (LA) and oleic acid (OA) by using functionalized mesoporous materials [4], zeolitic molecular sieves [5, 6], and solid cationic resins [7, 8] as catalysts. In another work, the beta-zeolite catalyst gave the conversion of fatty acids above 20% at optimum condition of glycerol : LA molar ratio of 1 : 1 at 100°C for 24 hours [9].

In this work, the usage and activities of the silicotungstic acid bulk (STAB) and the silicotungstic acid-silica sol-gel (STA-SG) have been studied. The STAB consists of two molecular structures, namely, Keggin and Dawson structures with four protons. The Dawson type STAB is formed by the combination of two Keggin molecules. The activity and stability of these catalysts depend on the structure and the type of the central atom along with the metal [10, 11]. The STAB is impregnated onto different supports such as polymers and silica [12] to achieve high surface area and stability in polar solvents.

2. Experimental

2.1. Synthesis of the Catalyst. The catalyst was prepared according to Izumi et al [13] methods with some modification. In this study, a mixture of water (2.0 mol), 1-butanol

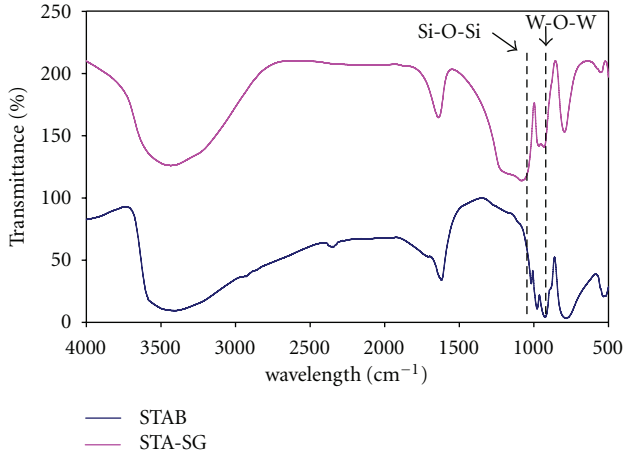

Figure 1: FTIR spectrum of STAB and STA-SG.

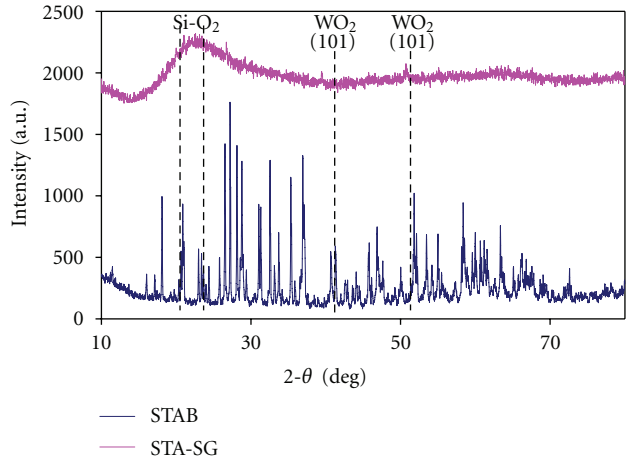

Figure 2: XRD diffractogram of STAB and STA-SG.

Table 1: BET surface area for STAB and STA-SG catalyst.

Type of catalyst	BET surface area (m^2/g)
STAB	0.98
STA-SG	460.12

(0.2 mol), and heteropoly acid ($5.0 \times 10-4$ mol) was added to tetraethyl orthosilicate (0.2 mol) and stirred at 80°C for 3 hours. Then, the hydrogel obtained was dehydrated slowly at 80°C for 1.5 hours. The dried gel obtained was extracted in sohxlet apparatus with methanol as a solvent for 72 hours and dried for overnight. The heteropoly acid immobilised silica was dried at 100°C for 3 hours to use as catalytic materials and characterized by using BET, FTIR, TEM, and XPS methods.

2.2. Characterization of the Catalyst. The Brunauer, Emmett dan Teller (BET) analysis of the STAB and STA-SG catalysts was applied by using Micromeritics model ASAP 2010 and the physical nitrogen adsorption was done at liquid nitrogen temperature of 77 K. The XRD method was performed by using XRD's Bruker AXS D8 Advance type with x-ray radiation source of Cu Kα (40 kV, 40 mA) to record the 2θ diffraction angle from 10° to 60° at wavelength ($\lambda = 0.154$ nm). TEM analysis was performed by using CM12 transmission electron microscope Philips type with electron gun at 200 kV. The X-ray photoelectron spectroscopy (XPS) measurement of the STAB and STA-SG catalysts were performed on XPS Axis Ultra from Kratos equipped with monochromatic Al Kα radiation. The samples were analyzed at the analysis chamber pressure at about 1×10^{-10} Pa. The spectra referenced with respect to C1s line at 284.5 eV.

2.3. Esterification Reaction. The esterification process between purified glycerol (from the palm oil transesterification source) and oleic acid was carried out in the batch reactor with STAB and STA-SG as the catalysts. The reaction was performed at 100°C for 8 hours and connected to the pump system in order to remove water during the reaction. The products were then separated from the unreacted reactants through centrifugation and analysed in the HPLC.

3. Results and Discussion

3.1. Physical Surface Analysis (BET). The analyses of BET showed that STAB has BET surface area of 0.98 m^2/g while STA-SG of 460.11 m^2/g as summarized in Table 1. The STA-SG catalyst gave a relatively higher surface area after sol-gel technique was applied. This could suggest that STA-SG has more active sites and high surface area towards higher activity and yield of GMO.

3.2. FTIR Analysis. The typical FTIR spectrum of STAB obtained at 1100 cm^{-1} (Si-O-Si), 968 cm^{-1} (W-O$_d$ terminal), 903 cm^{-1} (W-O$_b$-W edge shared) and 719 cm^{-1} (W-O$_c$-W) corner shared) corresponded to the primary structure $[SiW_{12}O_{40}]^{-4}$ of the catalyst [14] as can be seen in Figure 1. In the STA-SG catalyst, the Si-O-Si bond detected at 1100 cm^{-1} was bigger and wider than STAB catalyst. It clearly demonstrated that Si-O-Si bend with higher composition in STA-SG affected Si and O from TEOS and that STAB was chemically bonded with each other.

3.3. Catalysts Crystallinity by XRD. From XRD analysis, STAB sample generated many peaks which clearly shown that the sample was formed as crystalline compound. However, STA-SG obtained by sol-gel technique gave the amorphous state due to the presence of the silica compounds. From Figure 2, there was a broader peak shown at 28° which was represented by the Si-O-Si bond as the main component in STA-SG catalyst. Subsequently, this would lead to a predicted analysis by XPS that there would be nearly 50% Si-O-Si bond in STA-SG catalyst.

3.4. Surface Morphology by TEM. From Figures 3(b) and 3(c), TEM analysis has shown the morphology of STA-SG catalyst. The STAB was assorted in the silica based on TEOS. The distribution of the catalyst in silica phase was depicted in Figure 3(b). The STA-SG catalyst was smaller in size in

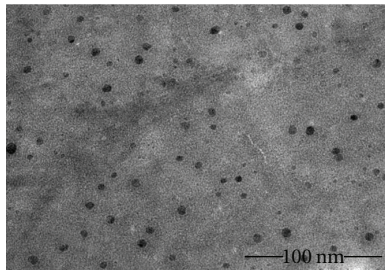

(a)

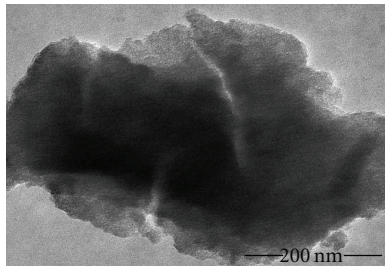

(b)

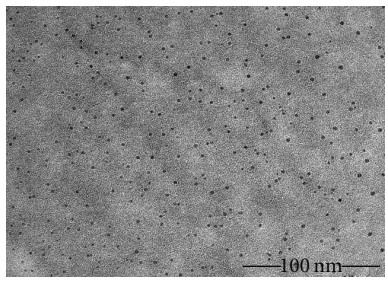

(c)

Figure 3: TEM micrograph for (a) STAB at 45KX, (b) STA-SG at 35KX, and (c) STA-SG at 45KX.

Table 2: Percentage of mass concentration (%) of C1s, O1s, Si2p and W4f elements from wide scan analyses for STAB and STA-SG catalysts.

Type of catalyst	C1s	O1s	Si 2p	W 4f
STAB	7.11	23.79	0.48	68.62
STA-SG	2.33	61.19	33.89	2.59

the range of 3.5–5.5 nm compared to STAB in the range of 17–20 nm.

From the analysis, it was noted that the equally shaped and smaller size of STA-SG particle was parallel to the BET characterization results that STA-SG has higher surface area compared to STAB. It was also affected by the additional of silica based on TEOS as sol gel technique.

3.5. Surface Analysis by XPS. The XPS investigation of binding energies (BE) and surface composition of silica supported STAB was investigated in detail. The XPS wide scan spectra of STAB and STA-SG was shown in Figure 4. The photoelectron peaks in the XPS spectra for STAB and STA-SG showed the presences of C1s, O1s, Si2p and W4f as expected. Percentages

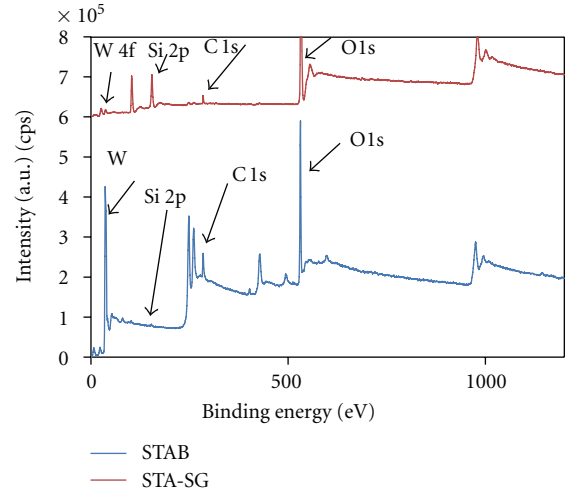

Figure 4: Wide scan for STAB and STA-SG.

of mass concentration for all the elements were summarized in Table 2.

From Figure 5(a), it was found that the bulk STA has Si2p binding energy at 102.5 and 103.3 eV, respectively. Meanwhile, the value of Si2p binding energy of STA-SG are 103.0, 103.7, and 104.5 eV (Figure 5(b)), indicating the formation of W-O-Si, Si-O-Si and $SiOH_2^+$, respectively. The Si2p-binding energy of 103.7 eV that represented of SiO2 was in agreement with the binding energy of silica found in the literature [15–18]. The O1s XPS narrow scan spectrum recorded from bulk STA was shown in Figure 6(a) and contained two distinct chemical states of O1s. This showed that the main (90.74%, 531.5 eV) and intermediate (9.26%, 532.8 eV) were the contributions of the presence of W-O-W and W-O-Si bonds, respectively [19].

The O1s spectra recorded from sample STA-SG (Figure 6(b)) was very different from the STAB (Figure 6(a)). The spectra consisted of the main signal at the 532.9 eV could be associated with Si-O-Si bond and a much weaker signals at the 532.1 and 533.7 eV, which might be represented by W-O-W and adsorbed water, $SiOH_2^+$. The W4f XPS spectra recorded from bulk STA (Figure 7(a)) composed of the spin-orbit doublet with binding energies for the $W4f_{7/2}$ and $W4f_{5/2}$ of 36.8 and 39.0 eV, respectively, with $\Delta BE = 2.13$. These values were typical of the presence of W (VI) [11]. The W4f spectra recorded from STA-SG is less well resolved than that of STAB (Figure 7(b)).

The W4f XPS also fitted on the basis of two different W contributions: a spin orbit doublet at 35.5 eV ($W4f_{7/2}$ component) which accounted for bigger area of the total spectra and a second doublet at 37.7 eV ($W4f_{5/2}$ component) accounting for the remaining area. The major component has a binding energy which was the same value as the STAB. The minor component appearing at the lower binding energy may represent the partial decomposition of STAB on the silica surface and the formation of an oxide of the type WO_x as WO_2 in which W has an oxidation state lower than VI.

Based on other researchers finding [16, 19], we suggest that there are a few interactions between $(H_3SiW_{12}O_{40})$—

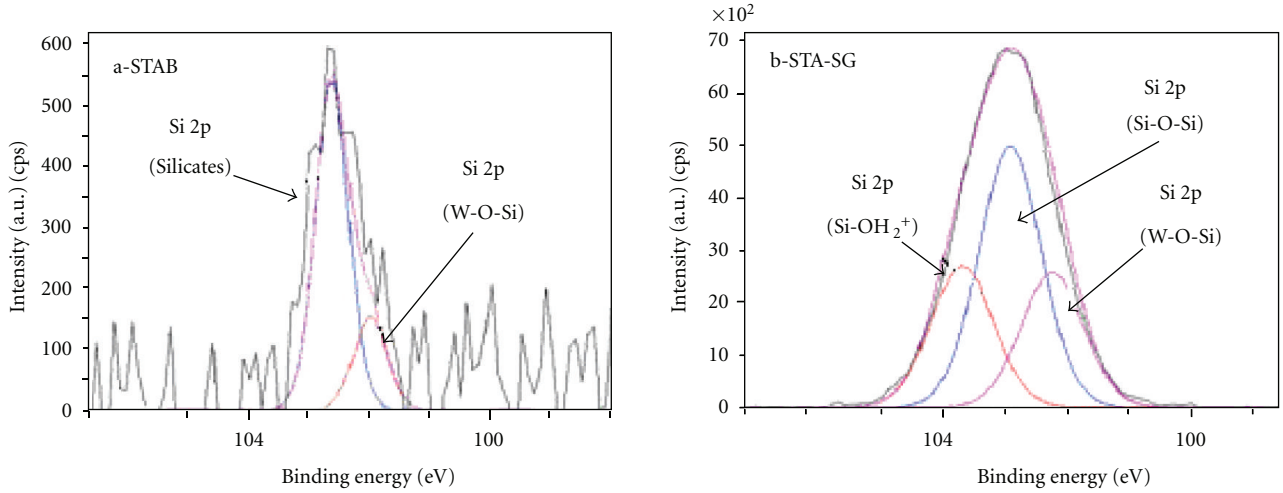

Figure 5: Narrow scan for Si2p (a) STAB and (b) STA-SG.

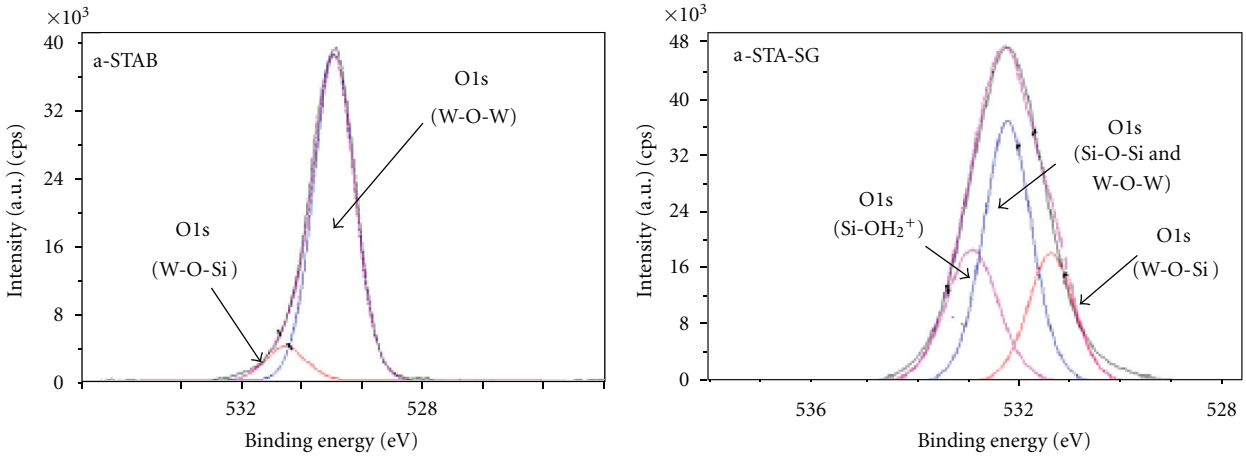

Figure 6: Narrow scan for O1s (a) STAB and (b) STA-SG.

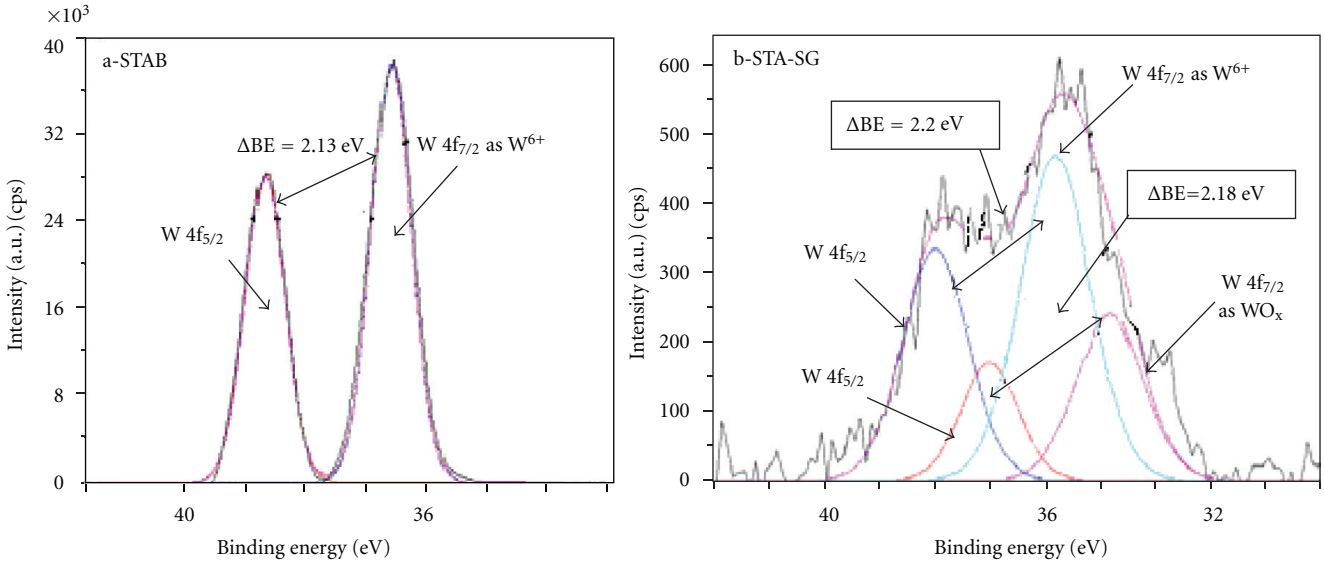

Figure 7: Narrow scan for W4f (a) STAB and (b) STA-SG.

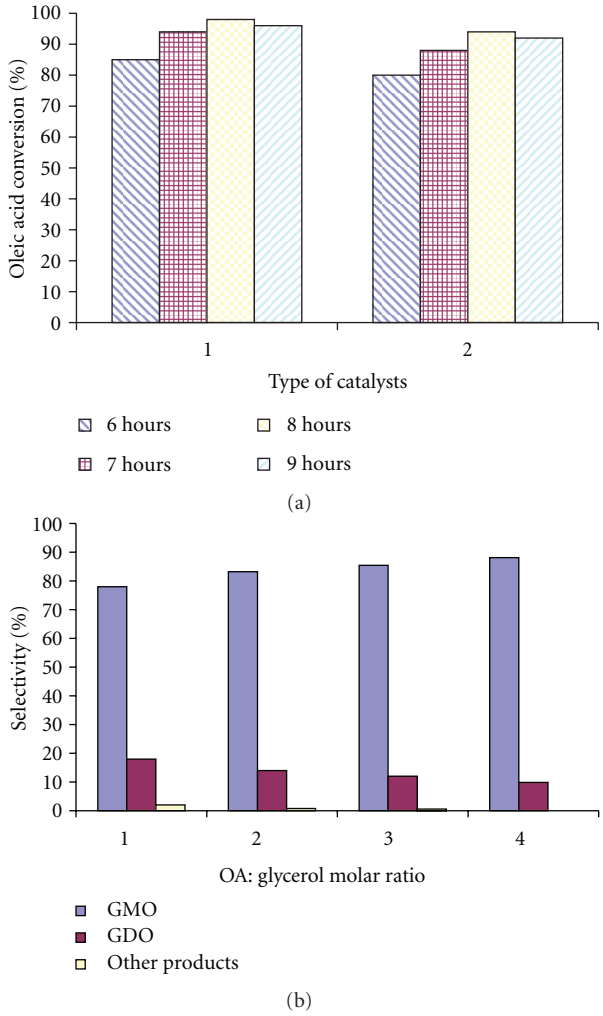

FIGURE 8: Catalytic activity in the esterification reaction (a) reaction time versus conversion for types of catalysts and (b) AO: glycerol molar ratio versus selectivity using STA-SG as the catalyst.

with the silanol groups at silica surface to give ion pairs in the form ($\equiv SiOH_2^+$) ($H_3SiW_{12}O_{40}$) from the reaction below: $\equiv$ Si-OH + $H_4SiW_{12}O_{40} \longrightarrow [\equiv$ Si-$OH_2]^+[H_3SiW_{12}O_{40}]^-$.

3.6. Esterification Reaction. The activity of the catalysts was studied based on the three main parameters, namely, reaction time, OA : glycerol molar ratio, and type of catalysts. From Figure 8(a), STAB gave a higher conversion of oleic acid with 98% compared to STA-SG with 96% at 100°C and OA : glycerol molar ratio of 6 : 1 for 8 hours. At 9 hours of the reaction, it was shown that the conversion was reduced to about 1.5%. This indicated that the backward reaction occurred because of the catalysts inhibition. However, the STA-SG catalyst gave relatively higher selectivity of the glycerol monoleate (GMO) and glycerol dioleate (GDO), the byproduct, of 95% and 5%, respectively. It was typically higher than STAB that gave selectivity to GMO and GDO of 89.9% and 10.1%, respectively.

The reaction temperature of 100°C was chosen to study the other parameters on the basis that the higher temperature would shift the reaction equilibrium to produce more side products such as GDO and acrolein but at a lower selectivity of GMO. However, the OA : glycerol molar ratio of 6 : 1 yielded higher selectivity of GMO of up to 95% at 100°C for 8 hours as depicted in Figure 8(b), hence the stronger parameter that promoted towards higher desired product. In other words, higher molar ratio of OA would increase the chances for higher GMO production, as the OA is three times easier to react with the glycerol compound.

4. Conclusion

The synthesized STA-SG catalyst that prepared by sol-gel technique has the good properties as well as catalytic materials. The H_2SO_4 and STAB catalysts gave higher conversion of 100% and 98% compared to STA-SG of 96%. Even though there were no significant differences among the three catalysts in terms of the conversion capability, the STA-SG catalyst has an advantage of enabling a higher selectivity of GMO with 95% compared to 89.9% and 81.6% by using STAB and H_2SO_4, respectively. This indicated that the solid heteropoly acid type STA-SG has a better catalytic activity and higher number of active sites that contributed towards higher selectivity of the main product, namely, glycerol monooleate (GMO).

Acknowledgments

The authors wish to thank Universiti Kebangsaan Malaysia (UKM) for funding this project under research Grant no. UKM-GUP-BTK-08-14-306 and Centre of Research and Innovation Management (CRIM).

References

[1] ATC Document 49. Lubricant Additives and the Environment, 2007.

[2] A. Corma, S. Iborra, S. Miquel, and J. Primo, "Catalysts for the production of fine chemicals: production of food emulsifiers, monoglycerides, by glycerolysis of fats with solid base catalysts," *Journal of Catalysis*, vol. 173, no. 2, pp. 315–321, 1998.

[3] N. O. V. Sonntag, "Glycerolysis of fats and methyl esters—status, review and critique," *Journal of the American Oil Chemists' Society*, vol. 59, no. 10, pp. 795a–802a, 1982.

[4] W. D. Bossaert, D. E. de Vos, W. M. van Rhijn et al., "Mesoporous sulfonic acids as selective heterogeneous catalysts for the synthesis of monoglycerides," *Journal of Catalysis*, vol. 182, no. 1, pp. 156–164, 1999.

[5] E. Heykants, W. H. Verrelst, R. F. Parton, and P. A. Jacobs, "Shape-selective zeolite catalysed synthesis of monoglycerides by esterification of fatty acids with glycerol," *Studies in Surface Science and Catalysis*, vol. 105, pp. 1277–1284, 1997.

[6] Z. Chen, J. Zhong, Q. Li, Y. Li, and Z. Ou, *Science in China Series B*, vol. 32, p. 769, 1989.

[7] S. Abro, Y. Pouilloux, and J. Barrault, *Comptes-Rendus de l'Académie des Sciences de Paris. Série II*, vol. 323, p. 493, 1996.

[8] S. Abro, Y. Pouilloux, and J. Barrault, "Selective synthesis of monoglycerides from glycerol and oleic acid in the presence of solid catalysts," *Studies in Surface Science and Catalysis*, vol. 108, pp. 539–546, 1997.

[9] M. D. S. Machado, J. Pérez-Pariente, E. Sastre, D. Cardoso, and A. M. de Guereñu, "Selective synthesis of glycerol monolaurate with zeolitic molecular sieves," *Applied Catalysis A*, vol. 203, no. 2, pp. 321–328, 2000.

[10] N. Mizuno and M. Misono, "Heterogeneous catalysis," *Chemical Reviews*, vol. 98, no. 1, pp. 199–217, 1998.

[11] G. Li, Y. Ding, J. Wang, X. Wang, and J. Suo, "New progress of Keggin and Wells-Dawson type polyoxometalates catalyze acid and oxidative reactions," *Journal of Molecular Catalysis A*, vol. 262, no. 1-2, pp. 67–76, 2007.

[12] D. Varisli, T. Dogu, and G. Dogu, "Novel mesoporous nanocomposite WO_x-silicate acidic catalysts: ethylene and diethylether from ethanol," *Industrial and Engineering Chemistry Research*, vol. 48, no. 21, pp. 9394–9401, 2008.

[13] Y. Izumi, K. Hisano, and T. Hida, "Acid catalysis of silica-included heteropolyacid in polar reaction media," *Applied Catalysis A*, vol. 181, no. 2, pp. 277–282, 1999.

[14] M. Aparicio, Y. Castro, and A. Duran, "Synthesis and characterisation of proton conducting styrene-co-methacrylate-silica sol-gel membranes containing tungstophosphoric acid," *Solid State Ionics*, vol. 176, no. 3-4, pp. 333–340, 2005.

[15] J. F. Moulder, P. E. Sobol, and K. D. Bomben, Eds., *Hand Book of X-Ray Photoelectron Spectroscopy (1992–1995)*, Physical Electronics Division.

[16] A. D. Newman, D. R. Brown, P. Siril, A. F. Lee, and K. Wilson, "Structural studies of high dispersion $H_3SiW_{12}O_{40}/SiO_2$ solid acid catalysts," *Physical Chemistry Chemical Physics*, vol. 8, no. 24, pp. 2893–2903, 2006.

[17] F. J. Berry, G. R. Derrick, J. F. Marco, and M. Mortimer, "Silica-supported silicotungstic acid: a study by X-ray photoelectron spectroscopy," *Materials Chemistry and Physics*, vol. 114, no. 2-3, pp. 1000–1003, 2009.

[18] T. Blasco, A. Corma, A. Martínez, and P. Martínez-Escolano, "Supported heteropolyacid (HPW) catalysts for the continuous alkylation of isobutane with 2-butene: the benefit of using MCM-41 with larger pore diameters," *Journal of Catalysis*, vol. 177, no. 2, pp. 306–313, 1998.

[19] A. D. Newman, A. F. Lee, K. Wilson, and N. A. Young, "On the active site in $H_3SiW_{12}O_{40}/SiO_2$ catalysts for fine chemical synthesis," *Catalysis Letters*, vol. 102, no. 1-2, pp. 45–50, 2005.